

Carbon aerogels through organo-inorganic co-assembly and their application in water desalination by capacitive deionization

Rudra Kumar^{1#}, Soujit Sen Gupta^{2#}, Shishir Katiyar¹, V. Kalyan Raman³, Siva Kumar Varigala³, T. Pradeep^{2*} and Ashutosh Sharma^{1*}

¹*DST Unit on Nanoscience, Department of Chemical Engineering, Indian Institute of Technology Kanpur 208016, India*

²*DST Unit on Nanoscience and Thematic Unit of Excellence (TUE), Department of Chemistry, Indian Institute of Technology Madras, Chennai 600036, India*

³*Centre of Excellence (Biotechnology) & Water and wastewater Technology, Thermax Limited, Pune 411019, India*

[#]*Both the authors contributed equally*

^{*}*Email: ashutos@iitk.ac.in; pradeep@iitm.ac.in*

Contents

N ₂ adsorption–desorption isotherm for pore size distribution of CA	Page 2
Compressive stress-strain curve for carbon aerogel	Page 3
Change in porosity with the change in concentration of the SiO ₂ precursor	Page 4
XPS survey spectrum of CSA	Page 5
SEM image and EDS of CSA	Page 6
CV curves of the carbon-silica aerogel	Page 7
Photograph of the CDI laboratory batch experimental set-up	Page 8
Rate of adsorption and kinetics for the CA material	Page 9
CDI performance of CA with different initial concentrations of NaCl	Page 10
XRD of CA before and after single adsorption cycle	Page 11
Decovoluted XPS spectrum of C1s and O1s after different cycles	Page 12

Supporting Information S1

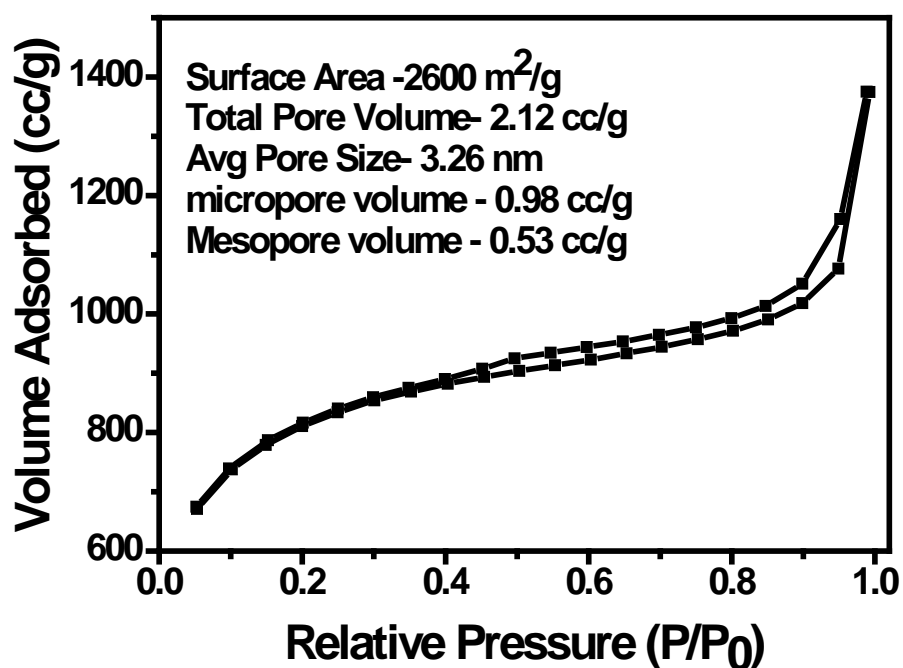


Fig. S1: N₂ adsorption–desorption isotherm and data of pore size distribution of CA.

Porosity measurement of CA sample shows that the total pore volume was 2.12 cc/g and average pore size was 3.26 nm. The pore size distribution (PSD) was obtained from the Barret-Joyner-Halenda (BJH) method.

The hysteresis in the curve at higher P/P₀ value shows the presence of large mesopores which arises due to the cross linking of smaller particles.

Supporting Information S2

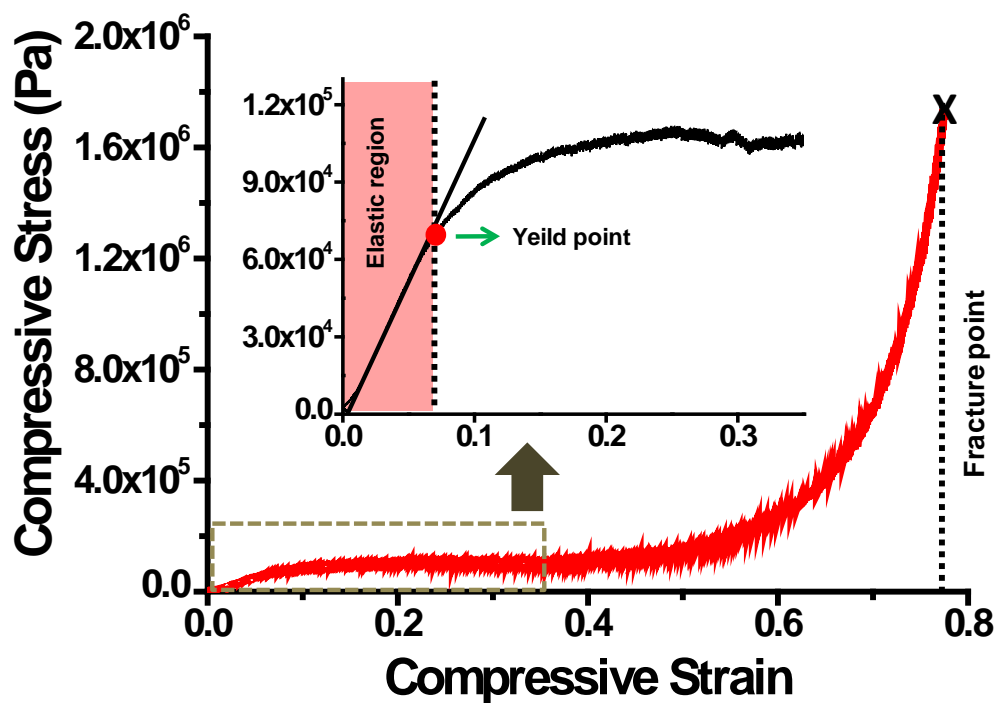


Fig. S2: Compressive stress-strain curve for carbon aerogel. The expanded region shows the elastic region and the yield point (marked). Fracture point is marked in the figure. The Young's modulus was calculated to be 1.12 MPa from the straight line (tangent) drawn in the elastic region.

Supporting Information S3

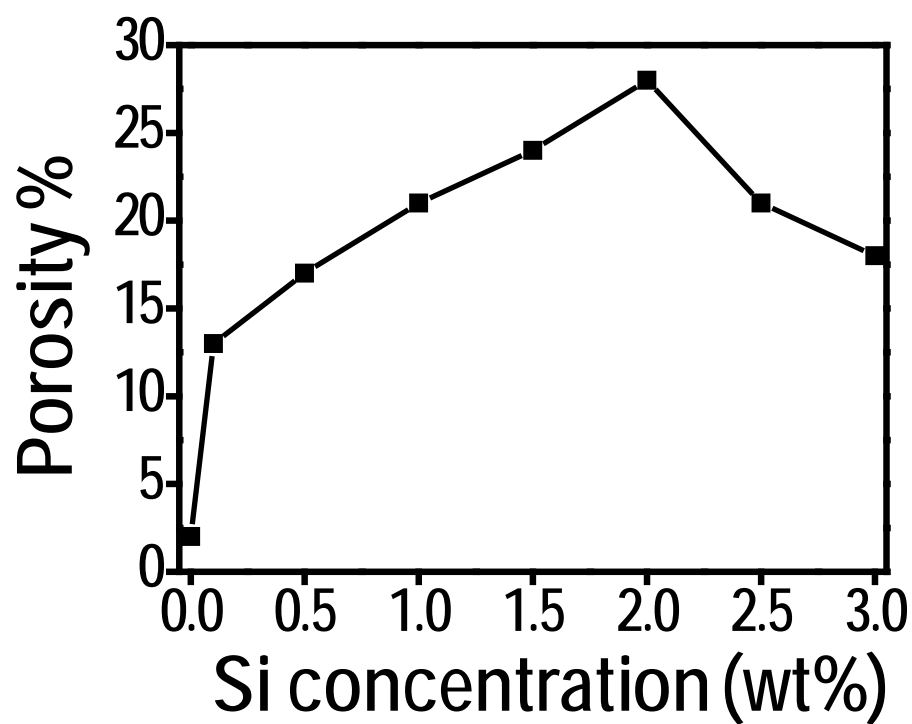


Fig. S3: Variation of porosity of CSA with the change in concentration of the SiO₂ precursor.

Supporting Information S4

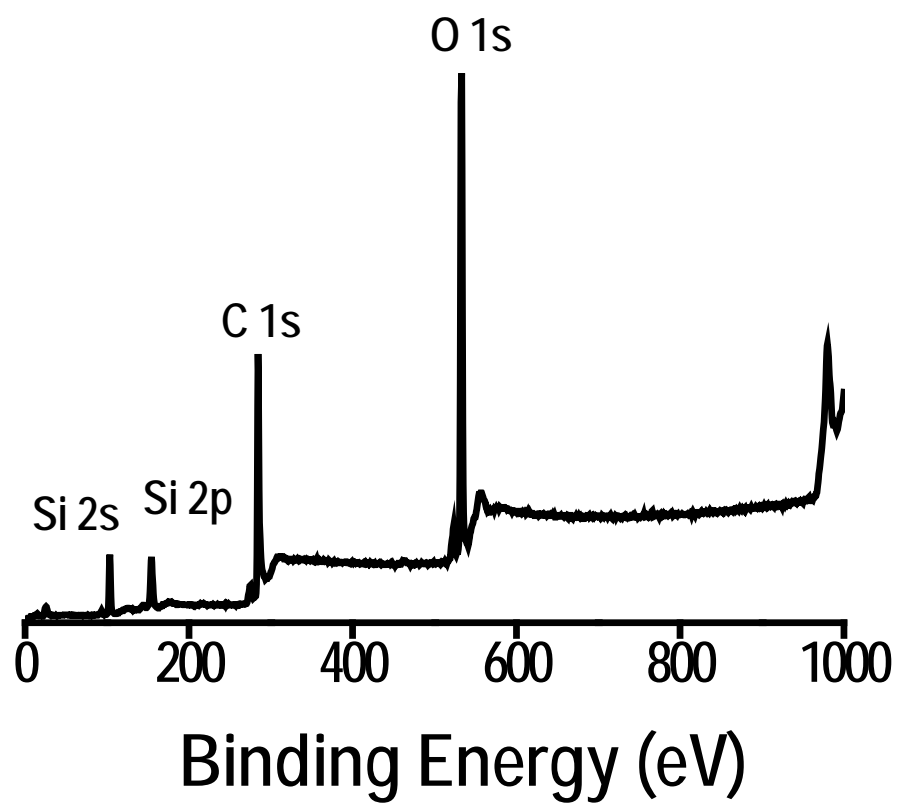


Fig. S4: XPS survey spectrum of CSA.

Supporting Information S5

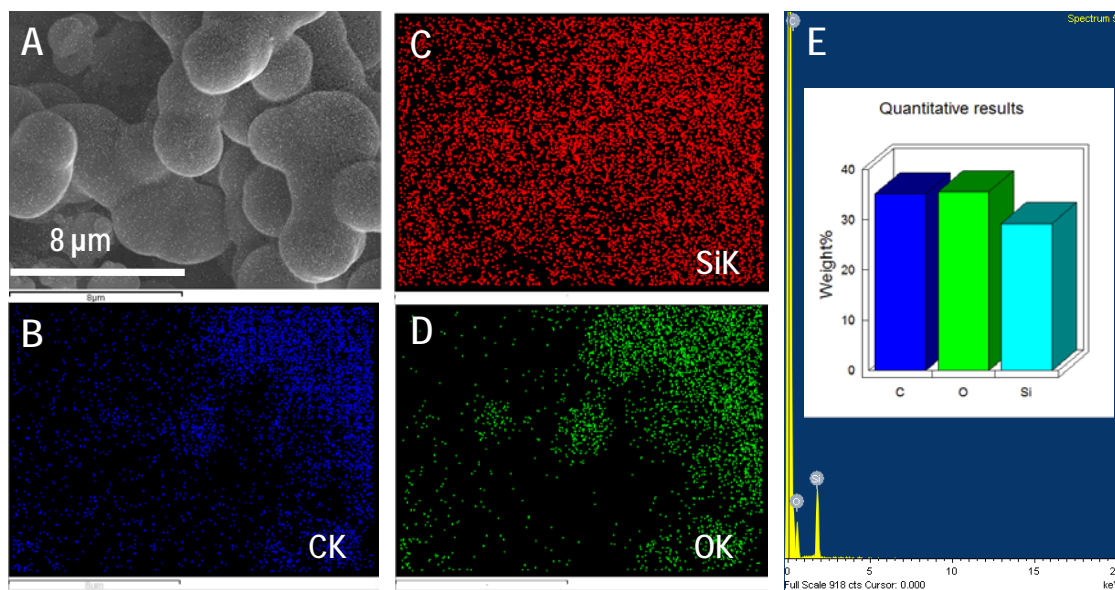


Fig. S5: A) SEM image of CSA B, C,D) EDS mapping of carbon, silica and oxygen and E)SEM-EDS with weight ratio of SiO₂ carbon aerogel.

Supporting Information S6

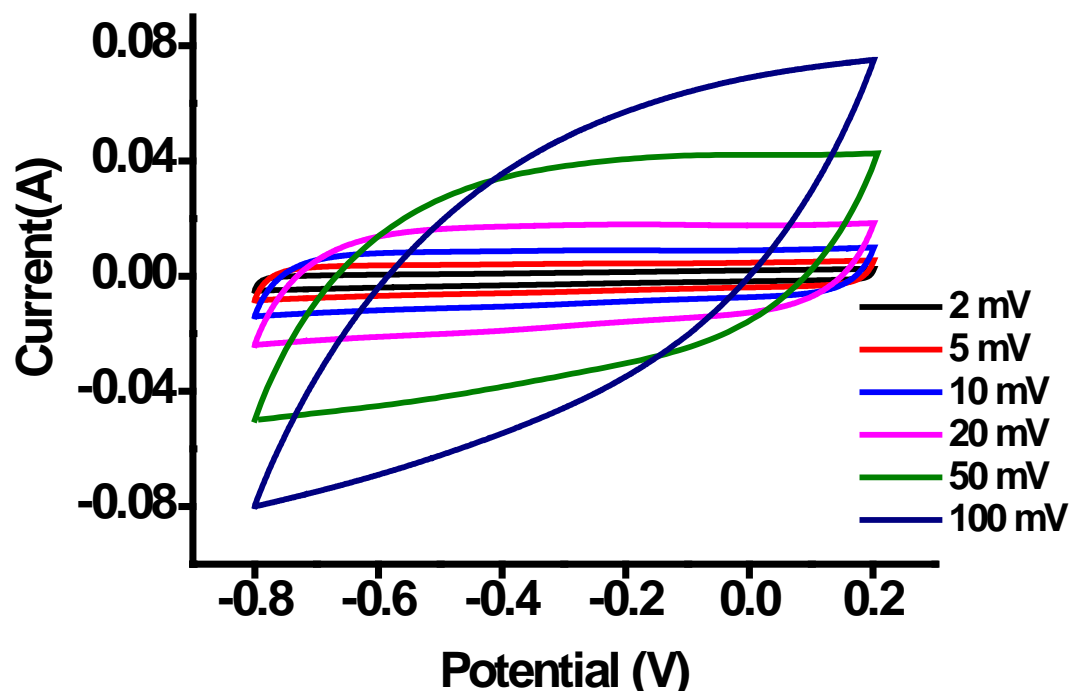


Fig. S6: CV curves of the carbon-silica aerogel at scan rates between 2 to 100 mV/s.

Supporting Information S7



Fig. S7: Photograph of the CDI laboratory batch experimental set-up.

Supporting Information S8

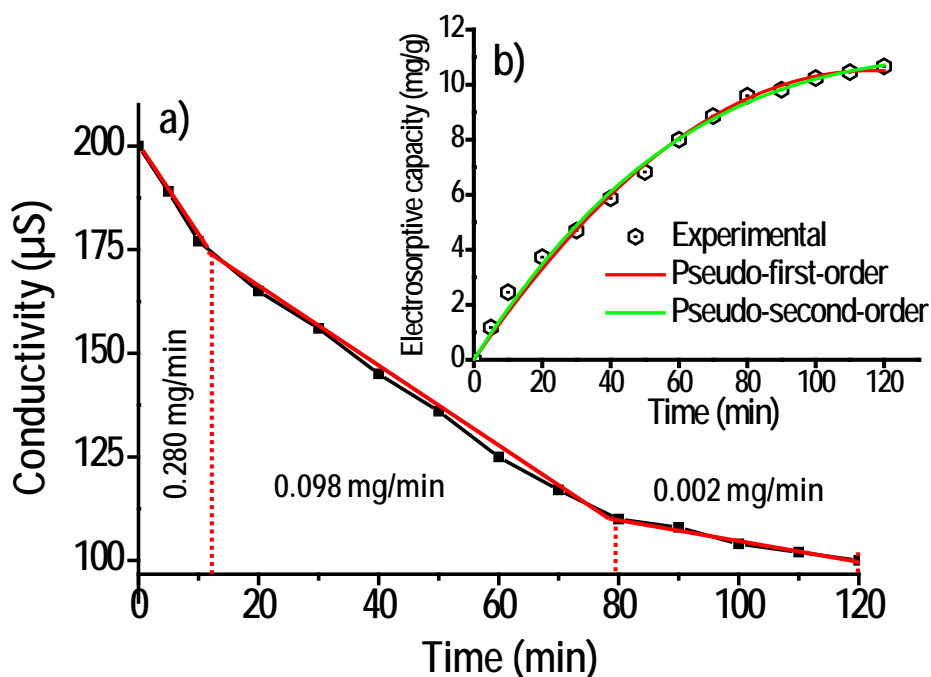


Fig. S8: a) Rate of adsorption for the CA material, having 200 ppm of NaCl solution. The kinetics shows a three step adsorption and b) represents the electrosorption kinetics for the CA electrodes and comparison with existing mathematical models.

The mathematical representations of the models are given below:

Pseudo-first-order equation:
$$q_t = q_e \left(1 - e^{-k_1 t}\right) \quad (1)$$

Pseudo- second-order equation:
$$q_t = \frac{q_e^2 k_2 t}{1 + q_e k_2 t} \quad (2)$$

Here, q_e and q_t (mg/g) denotes the amount of salt ion adsorbed at equilibrium and at time t (h), respectively. k_1 (1/h) and k_2 (g/mg h) are the first-order and second-order rate constants, respectively.

Supporting Information S9

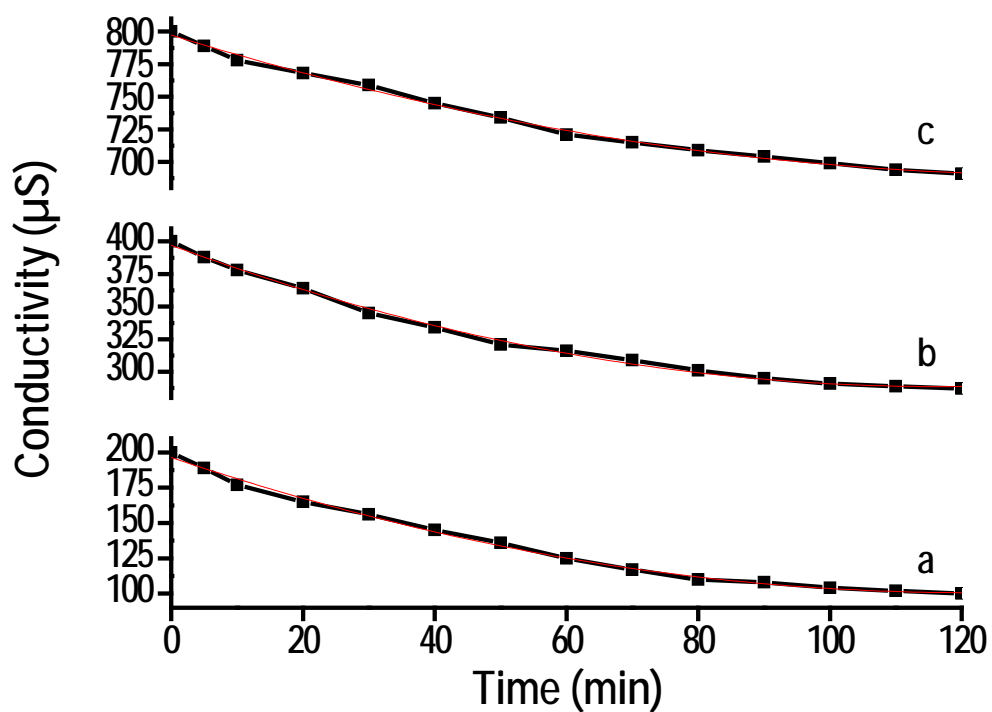


Fig. S9: CDI performance of CA with different initial concentrations of NaCl solution as electrolyte a) 200 ppm, b) 400 ppm and c) 800 ppm.

Supporting Information S10

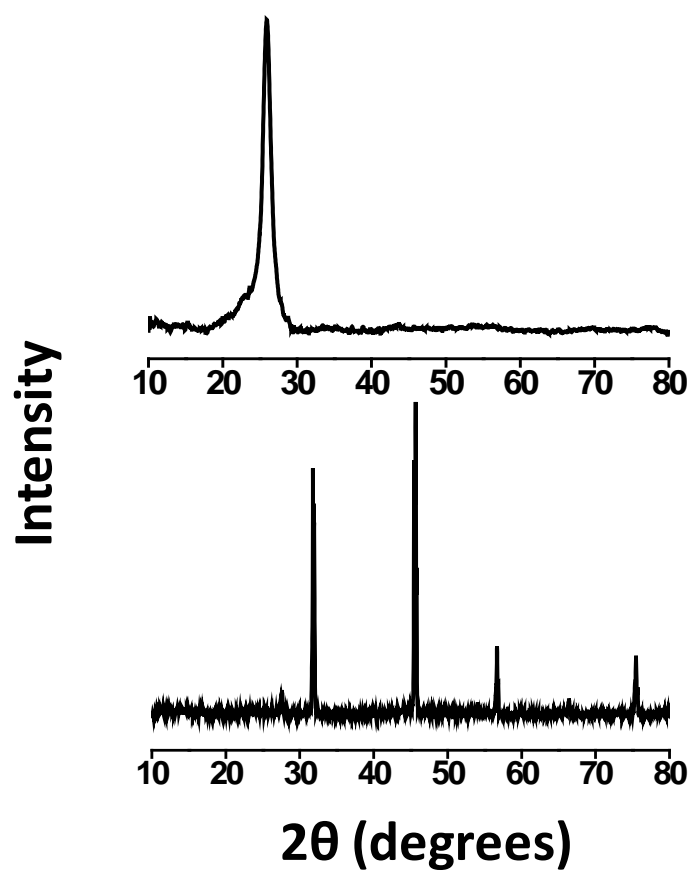


Fig. S10: XRD of CA A) before and B) after a single adsorption cycle.

Supporting Information S11

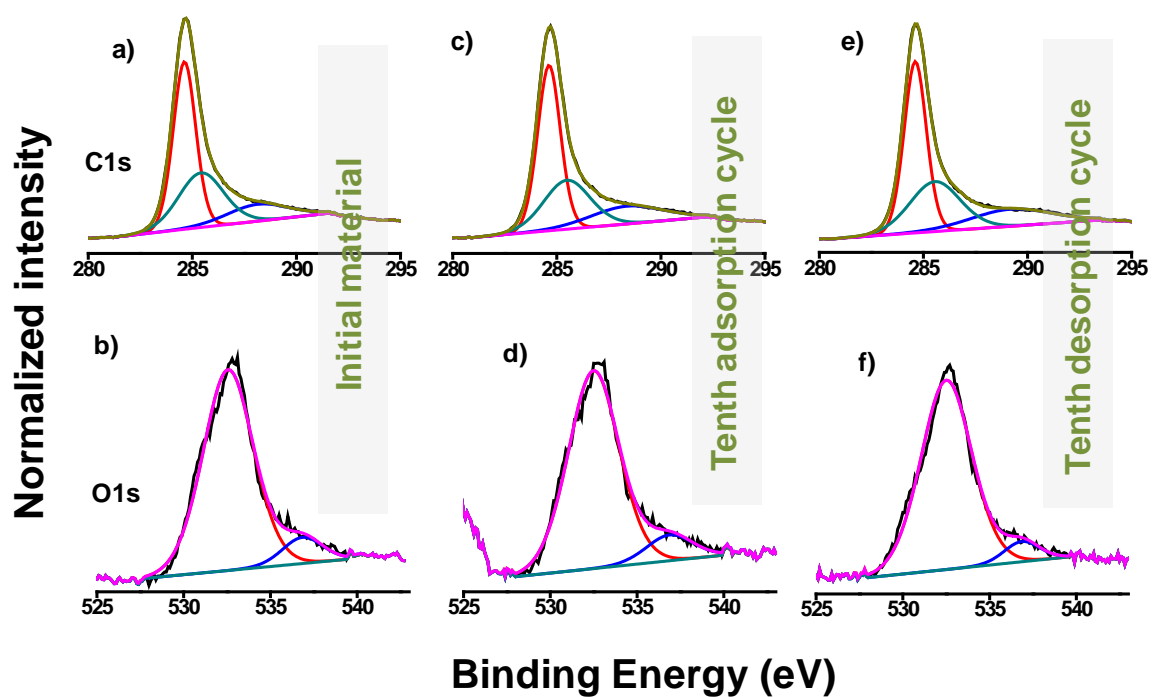


Fig. S11: Decoupled XPS spectrum of C1s and O1s, a & b) of pristine CA, c & d) after tenth adsorption cycle and e & f) after tenth desorption cycle. The corresponding XPS survey spectrum is shown in Figure 6A in the manuscript.